Closed Bipolar Electrodes for Spatial Separation of H_2 and O_2 Evolution during Water Electrolysis and the Development of High-Voltage Fuel Cells

Sean Goodwin, and Darren A. Walsh*

School of Chemistry and GSK Carbon Neutral Laboratory for Sustainable Chemistry

University of Nottingham

Jubilee Campus, Nottingham NG7 2TU, UK

E-mail: darren.walsh@nottingham.ac.uk;

Tel: 0044 115 8467495; Fax: 0044 115 9513562

Keywords: bipolar electrochemistry, electrocatalysis, hydrogen economy, electrolyser, regenerative fuel cell

Abstract

Electrolytic water splitting could potentially provide clean H_2 for a future 'Hydrogen Economy.' However, as H_2 and O_2 are produced in close proximity to each other in water electrolysers, mixing of the gases can occur during electrolysis, with potentially dangerous consequences. Herein, we describe an electrochemical water-splitting cell, in which mixing of the electrogenerated gases is impossible. In our cell, separate H_2- and O_2-evolving cells are connected electrically by a bipolar electrode in contact with an inexpensive dissolved redox couple ($K_3Fe(CN)_6/K_4Fe(CN)_6$). Electrolytic water splitting occurs in tandem with oxidation/reduction of the $K_3Fe(CN)_6/K_4Fe(CN)$ redox couples in the separate compartments, affording completely spatially-separated H_2 and O_2 evolution. We demonstrate operation of our prototype cell using conventional Pt electrodes for each gas-evolving reaction, as well as using earth-abundant Ni_2P electrocatalysts for H_2 evolution. Furthermore, we show that our cell can be run in reverse, and operate as a H_2 fuel cell, releasing the energy stored in the electrogenerated H_2 and O_2. We also describe how the absence of an ionically-conducting electrolyte bridging the H_2- and O_2-electrode compartments makes it possible to develop H_2 fuel cells in which the anode and cathode are at different pH values, thereby increasing the voltage above that of conventional fuel cells. The use of our cell design in electrolysers could result in dramatically improved safety during operation, and the generation of higher-purity H_2 than available from conventional electrolysis systems. Our cell could also be readily modified for the electrosynthesis of other chemicals, where mixing of the electrochemical products is undesirable.

Introduction

While renewable energy from wind turbines and solar panels offers obvious advantages over energy derived from fossil fuels, the diurnal and seasonal variability of renewable systems means that energy-storage systems are required to maintain a smooth energy supply. In principle, batteries could be used to store renewable electricity but, assuming costs remain stable for the foreseeable future, most grid-scale battery systems are too expensive (in \$ W^{-1}) for widespread adoption.[1] Mechanical storage of solar energy (for example, by pumping water uphill) is another attractive option but the requirements imposed by local geography are significant drawbacks.[2,3] An alternative approach is to use renewable energy to drive a thermodynamically-unfavorable reaction and store the energy in the chemical bonds of a liquid or gaseous fuel. If powered using renewable electricity, the generation of renewable H_2 from water is an extremely attractive option; the H_2 could be stored on site, and recombined with O_2 in a fuel cell to generate CO_2-free electricity on demand.[4] The generation of H_2 using renewable electricity would also have significant industrial implications; H_2 is a key reagent in the synthesis of commodity chemicals such as ammonia and methanol, but most of the world's H_2 is currently produced from fossil fuels, releasing CO_2 in the process.[5] The reactions involved in water electrolysis are given by either Equations 1 and 2, or 3 and 4 (depending on the pH of the electrolyser environment), giving the overall water-splitting reaction in Equation 5:

$$2H^+ + 2e^- \rightarrow H_2 \qquad E^0 = 0 \text{ V} \qquad (1)$$

$$H_2O \rightarrow \tfrac{1}{2}O_2 + 2H^+ + 2e^- \qquad E^0 = -1.229 \text{ V} \qquad (2)$$

$$2H_2O + 2e^- \rightarrow H_2 + 2OH^- \qquad E^0 = -0.828 \text{ V} \qquad (3)$$

$$2OH^- \rightarrow \tfrac{1}{2}O_2 + H_2O + 2e^- \qquad E^0 = -0.401\ \text{V} \qquad (4)$$

$$H_2O \rightarrow H_2 + \tfrac{1}{2}O_2 \qquad E^0_{\text{cell}} = -1.229\ \text{V} \qquad (5)$$

Alkaline-electrolyser technology, in which OH^- ions are transported between the electrodes through a liquid electrolyte, is relatively mature, and several commercial systems exist.[6,7] However, these systems generally have limited partial-load ranges, current densities, and operating pressures.[8] Proton-exchange membrane (PEM) electrolysers, in which H^+ ions are transported through polymeric electrolytes, offer a number of advantages over alkaline systems, including higher reaction efficiencies, operation at higher current densities, and lower operating costs.[8] In addition, PEM electrolysers can produce compressed H_2, and suffer from lower ohmic losses than alkaline systems, due to the use of thin (~30-150 μm) PEMs. A number of regenerative PEM electrolyser/fuel cell systems that can operate either in the electrolyser mode or the fuel-cell mode have also been developed, with the advantage that such systems can save space and/or cost (by requiring just a single device).[9]

A significant problem in all water electrolysers is that H_2 and O_2 are invariably evolved in proximity to each other, so transport of gases across the electrolyte, and in the headspace of high-pressure electrolysers, can occur, potentially resulting in the formation of explosive H_2/O_2 mixtures. Mixing of H_2 and O_2 in the presence of catalyst particles can also lead to the production of reactive oxygen species (ROS) that degrade PEMs.[10] While PEMs are more resistant than liquid alkaline electrolytes to gas crossover, crossover of gases through PEMs can occur, especially during high-pressure operation. The rate of gas crossover can be decreased by increasing the thickness of the PEMs or by using specialized composite PEMs, but each approach decreases membrane conductivity.[8,11,12] Recent efforts to prevent gas mixing in PEM electrolysers include the development of gas-impermeable, Li^+-

conducting ceramic electrolytes,[13] which transport Li^+ ions between two halves of the electrochemical cell during electrolysis. The Segré-Silberberg effect has also been used to control gas-bubble movement during electrolysis, minimising gas mixing at high currents, even in the absence of a membrane, but significant gas mixing occurred at low currents.[14] An alternative strategy is to decouple H_2 evolution and O_2 evolution completely, and a novel approach was reported by Cronin and co-workers who evolved H_2 and O_2 sequentially, using the polyoxometalate (POM) $H_3PMo_{12}O_{40}$ as a proton buffer. The POM took up protons released during O_2 evolution and then released them during H_2 evolution.[15-17] Another two-step electrolysis system was designed by Xia et al., who coupled H_2 and O_2 evolution to oxidation/reduction of a $Ni(OH_2)$ electrode.[18,19] Reduction of H_2O to H_2 was accompanied by oxidation of the $Ni(OH)_2$ electrode to NiOOH, and the subsequent O_2-evolution step was accompanied by reduction of NiOOH to $Ni(OH)_2$. Each of these systems offers a unique approach to temporal separation of H_2 and O_2 evolution, but the time for a complete electrolysis cycle and regeneration of the electrolysis system is obviously longer than for a system in which simultaneous H_2 and O_2 evolution can occur.

In this contribution, we describe an electrolytic system in which H_2 and O_2 evolution occur simultaneously, but mixing of the product gases is impossible. The key to our approach is the use of a closed bipolar electrode (CBE), which is a single electronic conductor in contact with two separate solutions, and at which anodic and cathodic reactions occur simultaneously.[20,21] While bipolar plates have been used for a long time to connect individual fuel cells and electrolysers in stacks, bipolar electrochemistry in a broader sense has received renewed interest in recent years, and is being used in electrochemical propulsion,[22] sensors[20,23] and for monitoring the long-term electrocatalytic activity of anodic and cathodic half-cell reactions during water electrolysis.[24] We demonstrate here a novel cell design, in

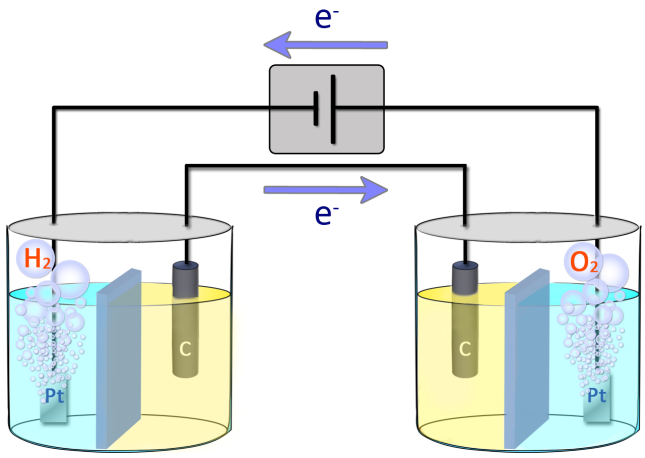

Figure 1. Water-electrolysis cell containing a closed bipolar electrode.

which CBEs are used in conjunction with reversible solution phase redox species to effect sustained, spatial separation of H_2 and O_2 during water electrolysis. A schematic of our system is shown in Figure 1. Each cell contains a Pt electrode, which is immersed in 0.1 M KOH and connected to an external power source. The CBE comprises a carbon cloth electrode immersed in each cell, connected by a wire. In each cell, the carbon is in contact with 0.1 M KOH containing an electrochemically-reversible redox species ($K_3Fe(CN)_6/K_4Fe(CN)_6$). The redox species are separated from the pure KOH solutions by Nafion membranes, to hinder access of the $Fe(CN)_6^{3-}/Fe(CN)_6^{4-}$ species to the Pt electrodes. During electrolysis, O_2 is produced at the Pt surface in the right-hand cell and H_2 is produced in the left-hand cell. In a conventional electrolyser, an electrolyte solution or membrane would connect the two sides of the cell to each other, completing the circuit by ion transfer between the cell compartments. However, in our cell, $Fe(CN)_6^{3-}/Fe(CN)_6^{4-}$ reduction/oxidation occurs at each end of the carbon-cloth CBE to complete the electrochemical circuit, meaning that gas crossover between the cells cannot occur. From left to right in Figure 1, the half reactions occurring at each electrode/electrolyte interfaces are as follows:

$$2H_2O + 2e^- \xrightarrow{\text{Pt}} H_2 + 2OH^- \quad (6)$$

$$2[Fe(CN)_6]^{4-} \xrightarrow{\text{C cloth}} 2[Fe(CN)_6]^{3-} + 2e^- \quad (7)$$

$$2[Fe(CN)_6]^{3-} + 2e^- \xrightarrow{\text{C cloth}} 2[Fe(CN)_6]^{4-} \quad (8)$$

$$2OH^- \xrightarrow{\text{Pt}} \tfrac{1}{2}O_2 + H_2O + 2e^- \quad (9)$$

In order to continually run the device as a water electrolyser, the anode and the cathode can be periodically switched (i.e. hydrogen can be evolved alternately at the left and right hand Pt electrode), maintaining the pH of the electrolytes, and regenerating the $[Fe(CN)_6]^{3-}/[Fe(CN)_6]^{4-}$ redox species. As we show below, the device can also be run as a fuel cell, which releases the energy stored in the electrogenerated gases and regenerates the $[Fe(CN)_6]^{3-}/[Fe(CN)_6]^{4-}$ redox species. In addition, as the catholyte and anolyte in our system cannot mix, we demonstrate that cell voltages >1.229 V can be achieved by using different-pH electrolytes in each compartment, an approach that cannot be achieved using conventional devices.

Results and Discussion

Electrolysis of Water in CBE System. Figure 2 shows photographs of a CBE system before and after 3.7 V was applied between the Pt electrodes for 3×10^3 s (much lower potentials are required for water splitting; a high voltage was used here for demonstration purposes). Inverted glass tubes containing the respective electrolytes were placed over each

electrode (Figure 2A). When the voltage was applied, bubbles formed at each Pt electrode and displaced the solutions (Figure 2B). However, no bubbles were evolved from the CBE when the voltage was applied (a video of the experiment is available in the supporting information). Figure 3A shows that the quantity of H_2 produced increased linearly up to 5×10^3 s, and increased as the voltage was ramped from 2.0 V to 2.6 V. Correlation of the quantity of H_2 produced with the charge passed during electrolysis showed faradaic efficiencies up to 80%. It was not possible to ensure that no gases leaked from our prototype cell during measurements of the gas volumes, so these high measured efficiencies suggest that quantitative gas evolution occurred during electrolysis.

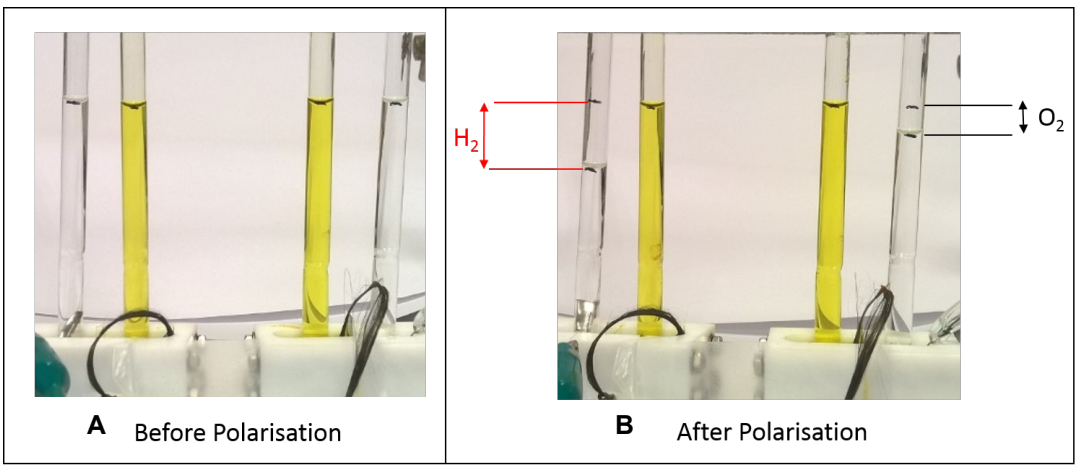

Figure 2. CBE system (A) before and (B) after 3.7 V was applied between the Pt flag electrodes for 3×10^3 s. The glass tubes were filled with 0.1 M KOH (far left and far right), and 0.1 M KOH containing 0.25 M $K_3Fe(CN)_6$ and 0.25 M $K_4Fe(CN)_6$ (centre left and centre right, respectively).

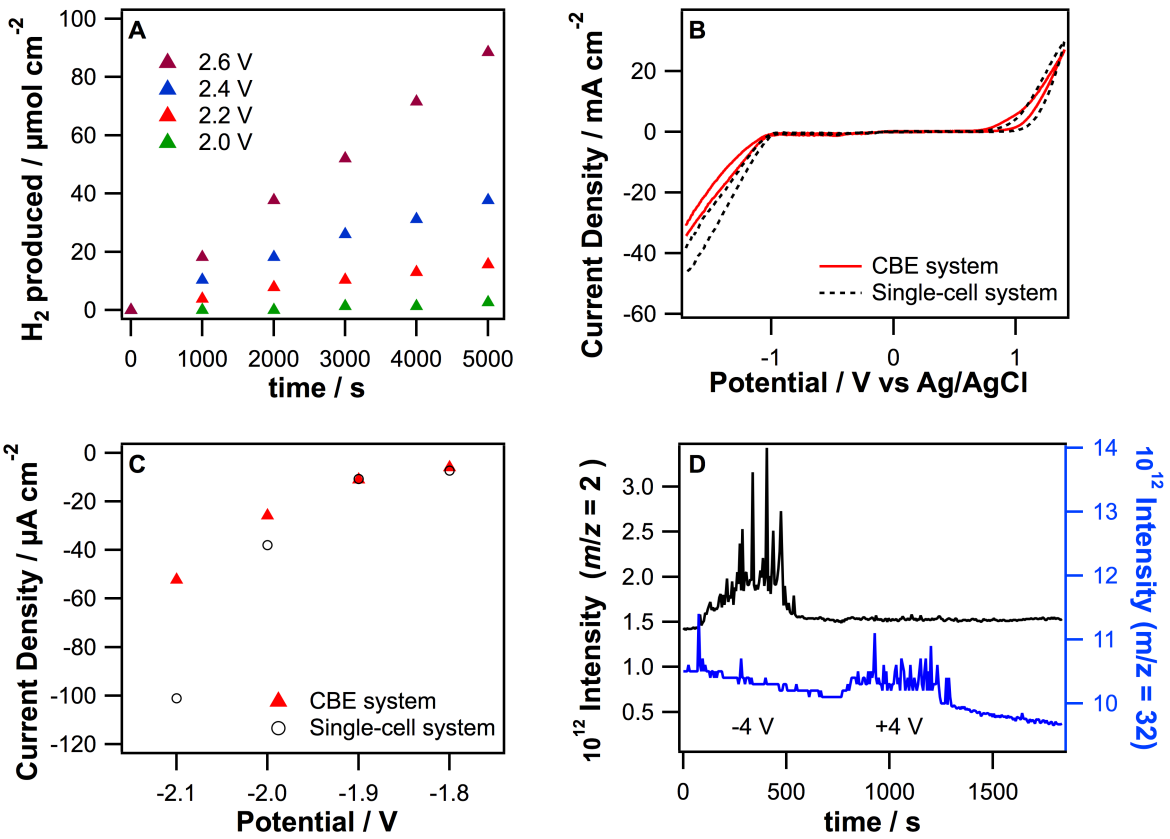

Figure 3. (A) Amount of H_2 produced from the Pt cathode of a CBE system as a function of time, and at a range of voltages, using a Pt-wire working electrode (3.8 cm length) and a Pt flag counter electrode. Amounts are normalized to the surface area of the working electrode. (B) Cyclic voltammogram recorded at a Pt disk working electrode in a single electrochemical cell containing 0.1 M KOH, a Pt flag counter electrode, and Ag/AgCl reference electrode (dashed line). The potential was cycled between −1.7 V (initial potential) and 1.4 V at 50 mV s^{-1}. The solid line shows a voltammogram recorded using the same working, counter and reference electrodes, but using the CBE system shown in Figure 1. The Ag/AgCl reference electrode was in the right-hand cell of the CBE system, along with the counter electrode, and the working electrode was in the left-hand cell. (C) Electrolysis current densities flowing in CBE and single-cell systems as a function of the applied potential. Pt-disk electrodes were used as the working electrode and the counter electrode. (D) m/z = 2 and m/z = 32 mass spectrometer signals recorded as a function of time after attaching the inlet of a mass spectrometer to a CBE system. −4.0 V was applied to the cell in the time range 56 s < t < 467 s and +4.0 V was applied in the range 740 < t < 1238 s.

To study the effect of using the CBE on the electrolysis reactions further, a conventional electrochemical cell containing a Pt working electrode, a Pt counter electrode, and an Ag/AgCl reference electrode was charged with aqueous KOH, and water electrolysis

in this cell was compared with that in the CBE system. The black dashed line in Figure 3B shows the cyclic voltammogram recorded when the potential of the Pt working electrode was cycled between −1.7 and +1.4 V vs. Ag/AgCl. At potentials positive of approximately 0.6 V, an anodic current flowed due to O_2 evolution at the Pt surface, and at potentials negative of about −1.0 V, a cathodic current flowed due to H_2 evolution. The potential difference between the onsets of H_2 evolution and O_2 evolution was therefore about 1.6 V, which is typical of that expected for water splitting using Pt electrodes.[25] This voltammogram can be compared with that recorded using the CBE system (red line of Figure 3B). The cell was set up as shown in Figure 1, but with an Ag/AgCl reference electrode immersed in the right-hand cell. The same Pt electrodes were used in the single electrochemical cell and CBE system, and H_2 and O_2 evolution occurred in each system at the same potentials. However, the current flowing in the CBE-containing cell was slightly lower than in the conventional cell. For example, the current flowing at −1.4 V in the CBE cell was 67% of that flowing at the same potential in the single cell. Figure 3C shows the electrolysis currents flowing after 90 s of electrolysis using the CBE system and a single electrochemical cell containing Pt working and counter electrodes. At high overpotentials, there was a considerable difference in the electrolysis currents; the current in the CBE system was 52% of that in the single electrochemical cell at −2.1 V due to additional resistance introduced by using the CBE. However, at low overpotentials the currents recorded in the single-compartment and CBE systems were the same within experimental error.

Purity of the Electrogenerated H_2. A mass spectrometric experiment was undertaken to determine whether the gases evolved in the CBE system were completely spatially separated. Ar gas was flowed through one cell of the CBE system, to carry electrolysis products from the cell through an outlet tube and to a mass spectrometer. The electrode in the cell attached to the outlet tube was first polarized at −4.0 V and then at +4.0 V, and the

resulting mass spectrometric traces are shown in Figure 3D. When the electrode was polarized negative, an increase in the H_2 (m/z = 2, black trace) signal was observed. Initially some O_2 (m/z = 32, red trace) was also observed as ambient O_2 in the cell solution was displaced by H_2, but this signal quickly decayed to the background while sustained H_2 evolution was observed. When the polarity of the cell was reversed, O_2 was detected from the cell, but no H_2 was observed above the background signal, confirming that spatially-separated H_2 and O_2 evolution was achieved using the CBE system.

Hydrogen Evolution Using Earth Abundant Catalysts. As well as mitigating effects such as gas crossover in water electrolysers, another challenge in the development of water electrolysers is the discovery and development of sustainable materials for these devices. Pt-group metals are the electrocatalysts of choice for evolution of H_2 and O_2 in these devices, and many researchers are focused on the development of lower cost, earth-abundant transition-metal electrocatalysts for these reactions.[26-29] Ni_2P has shown particularly high electrocatalytic activity for H_2 evolution, and we tested whether this electrocatalyst could be used for H_2 evolution in our system.[30-32] Figure 4A shows an X-ray diffraction pattern of the Ni_2P deposited on the electrode, confirming that the material was Fe_2P-type Ni_2P,[31] and the SEM images in Figures 4C and 4D show that the Ni_2P was formed of microscopic particles. Figure 4B shows polarization curves recorded using glassy carbon (GC), Ni_2P/GC (Ni_2P loading = 0.16 mg cm^{-2}), and Pt working electrodes in single electrochemical cells containing Ag/AgCl reference electrodes and Au counter electrodes (dashed lines). The solid lines show the polarization curves recorded using a CBE system with a Pt, glassy carbon, or Ni_2P/glassy carbon electrode in one cell, and an Ag/AgCl reference electrode and Au counter electrode in the other cell. When the single-cell system contained Pt as the H_2-evolution electrocatalyst (dashed red line), the H_2-evolution onset potential was approximately −0.95 V. When the electrode was changed to the GC electrode, the onset potential changed to

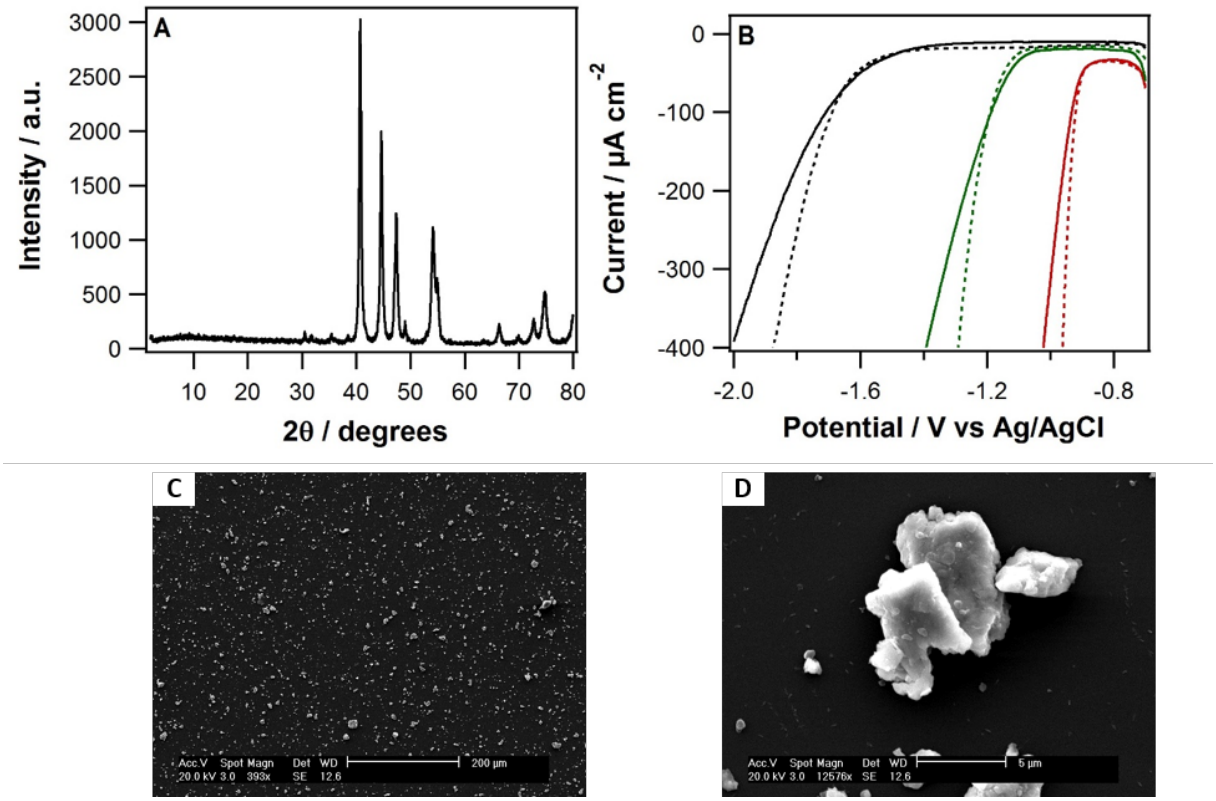

Figure 4. (A) Powder X-ray diffraction pattern of Ni_2P. (B) Polarization curves (dashed lines) recorded using a single electrochemical cell containing an Ag/AgCl reference electrode, an Au counter electrode, and either a glassy carbon (black), platinum (red) or Ni_2P/glassy carbon (green) working electrode. The solid lines show the curves recorded using the CBE system containing an Au counter electrode and Ag/AgCl reference electrode in the right-hand cell and a Pt, glassy carbon, or Ni_2P/glassy carbon electrode in the left-hand cell. Potentials were swept negative at 5 mV s^{-1} from −0.7 V. (C and D) SEM images of the Ni_2P powder.

approximately −1.6 V, and then to −1.1 V when using the Ni_2P electrodes. The remarkable activity of the Ni_2P electrode, which catalyses H_2 evolution at an onset potential about 150 mV more negative than at Pt, has been observed previously.[30] When each electrode was incorporated into the CBE systems (solid lines in Figure 4B), the H_2-evolution overpotential increased slightly in each case due to resistances within the cell (for example, the overpotential difference was approximately 10 mV at 200 μA cm^{-2} when using the Pt electrocatalyst). However, it is clear from Figure 4B that the CBE system can operate with

the earth-abundant H_2-evolution electrocatalyst, and the difference in overpotential observed when using the CBE and the single electrochemical cell systems is small. Of course, our system requires the use of a membrane in each of compartment of the cell, rather than just a single membrane separating the H_2 and O_2-evolving cells in a conventional PEM electrolyser. However, the advantage of our approach is that the two cells are separated by an electrical conductor and not simply a membrane, so gas mixing becomes impossible. It is important to note that, despite that fact that the conductivity of the neutralized Nafion membranes in the alkaline medium is more than two orders of magnitude smaller than that of acidified Nafion (3×10^{-5} S cm^{-1} in 0.1 M KOH *vs.* 9×10^{-3} S cm^{-1} for the acidified form, as measured using impedance spectroscopy), the Nafion membranes did not cause very large overpotentials during operation of the cell. Furthermore, the Nafion membranes retained their robustness during operation, and prevented access of $Fe(CN)_6^{3-}$/$Fe(CN)_6^{4-}$ ions to the Pt electrodes over the course of the electrolysis (~1-2 hr). For future iterations of the CBE cell, it would be advantageous to identify redox mediators that are electrochemically inactive at the H_2 and O_2-evolving electrodes, so membranes to isolate these electrodes from the mediators actually become unnecessary.

Decoupled H_2 and O_2 Oxidation in Fuel Cells containing a CBE. An energy-storage device is only useful if the stored energy can be recovered (for example, after sunset or when the wind stops blowing, and alternative-energy resources become ineffective). To demonstrate that our cell could be run in reverse and used as a fuel cell, which releases the energy stored in the electrogenerated H_2, voltammetry was carried out using the system after saturation of the electrolytes with H_2 and O_2. The red lines in Figure 5A and 5B show voltammograms recorded using the system when the electrolyte in the left-hand cell was saturated with H_2 (Figure 5A) and subsequently with O_2 (Figure 5B). The black dashed line

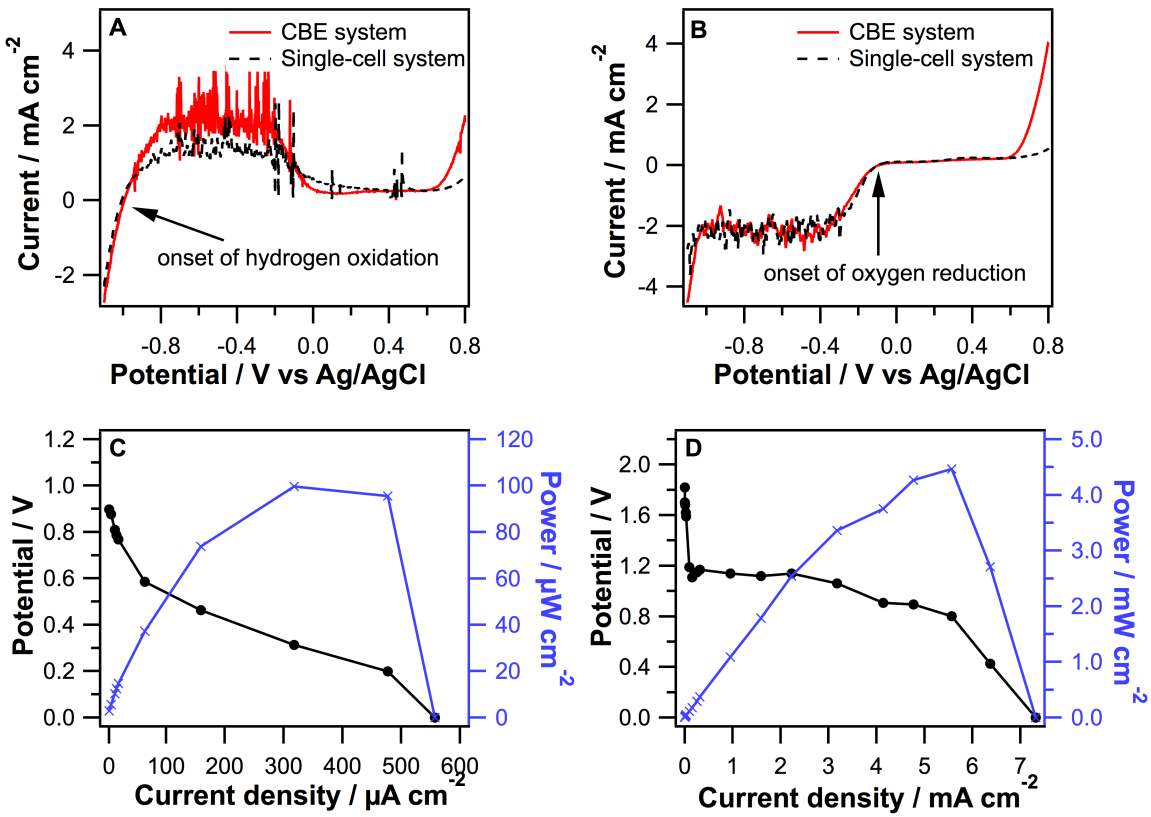

Figure 5. Linear sweep voltammograms recorded in stirred (A) H_2-saturated and (B) O_2-saturated 0.1 M KOH using a 2-mm diameter Pt working electrode in (dashed black lines) a single electrochemical cell and (solid red lines) a CBE system. A Pt flag was used as the counter electrode, and potentials were swept positive from −1.1 V vs Ag/AgCl at 50 mV s^{-1}. When using CBE systems, the reference electrode was in the cell opposite to that of the working electrode. (C) Polarization curve (black markers) recorded using the CBE system, while O_2 and H_2 bubbled over the working and counter electrodes respectively. The calculated power-potential graph is shown by the blue markers. (D) Polarization curve (black markers) recorded using a CBE system in which the catholyte and anolyte contain 1.0 M H_2SO_4 and 1.0 M KOH, respectively (the complete cell configuration is as described in the text.) The calculated power-potential graph is shown by the blue markers.

in each voltammogram shows the response obtained using a single electrochemical cell system when the electrolyte was saturated with H_2 and O_2, respectively. Figure 5A shows that an anodic current for the H_2-oxidation reaction (HOR, Equation 10) began to flow in each system at approximately −0.9 V as the potential was swept positive in the H_2-saturated solutions. Steady HOR currents then flowed as the potential increased before the current decreased to zero as the Pt surface became oxidized (at about 0 V vs. Ag/AgCl). Therefore,

the HOR proceeded at similar rates at all potentials in the single cell and the CBE system. Figure 5B shows that the O_2-reduction reaction (ORR, Equation 11) also proceeded at similar rates in each system; the cathodic ORR current increased from about −0.1 V as the potential was swept negative and reached approximately steady-state values at potentials negative of −0.4 V. Therefore, the difference in HOR and ORR onset potentials was approximately 0.8 V, as expected from previous studies of the HOR and ORR.[33]

$$H_2 + 2OH^- \rightarrow 2H_2O + 2e^- \qquad E^0 = 0.828 \text{ V} \qquad (10)$$

$$\tfrac{1}{2}O_2 + H_2O + 2e^- \rightarrow 2OH^- \qquad E^0 = 0.401 \text{ V} \qquad (11)$$

Polarization curves were recorded by increasing the current flowing through the CBE system while O_2 and H_2 were bubbled over the cathode and anode, respectively, while each electrolyte was stirred at 300 rpm (the system was otherwise similar to that shown in Figure 1). Figure 5C shows an initial sharp decrease in potential from about 0.9 V to about 0.6 V as the current increased, due to activation losses. An approximately linear drop in potential from 0.6 V to 0.2 V was observed as the current increased from 80 to 480 μA cm^{-2}, due to ohmic losses in the cell, and finally a sharp drop in potential was observed at the highest current, due to mass transport losses. The general shape of this polarization curve is similar to that recorded using conventional H_2 fuel cells.[34] The potential-power density curve is shown in blue, and shows that a maximum power of about 100 μW cm^{-2} was delivered by the CBE system. These results show that not only can the CBE system run as an electrolyser, it can also run in reverse as a fuel cell. Of course, relatively low peak power was produced by our proof-of-principle prototype device due to, for example, the use of polished, smooth disk

electrodes and cells that were not gas-tight, but such factors can readily be optimized in future iterations of our cell design.

Mixed pH Closed-Bipolar Electrode Fuel Cell System. The half-cell reactions occurring in conventional fuel cells are the reverse of Equations 1 and 2 (when the electrolyte is acidic) or Equations 10 and 11 (when the electrolyte is alkaline), giving a theoretical maximum (thermodynamic) cell potential of 1.229 V. Note that the actual voltage of H_2 fuel cells is significantly lower than this value at all currents due to activation, ohmic, and mass-transport losses within the cells (as is also shown in Figure 5C).[35] However, by separating two electrolytes using a CBE, it is possible to use electrolytes with different pH values to increase the cell potential to a value higher than achievable using a single electrolyte. If the left-hand cell (the cathode) contains O_2 bubbled through a solution at pH = 0 and the right-hand cell contains H_2 bubbled through a solution at pH = 14, the overall reaction is described by Equation 12 (which is a combination of the reverses of Equations 2 and 3), giving a higher cell voltage than possible in a single-pH device.[36]

$$H_2 + ½O_2 + H^+ + OH^- \rightarrow 2H_2O \qquad E^0_{cell} = 2.057\ V \qquad (12)$$

To avoid contact of $Fe(CN)_6^{3-}/Fe(CN)_6^{4-}$ with an acidic electrolyte, a different CBE to that described above was used to construct our mixed-pH cell. Ag/AgCl electrodes, in which the potential-determining equilibria are as shown in Equation 13, were used, giving the overall cell notation $Pt|O_2|$1.0 M KCl, 1.0 M $H_2SO_4|AgCl,Ag,AgCl|$1.0 M KCl, 1.0 M $KOH|H_2|Pt$.

$$AgCl + e^- \rightarrow Ag + Cl^- \qquad (13)$$

To construct our prototype fuel cell, a silver plate, which had been electrolytically coated on both sides with AgCl, was used as the CBE. O_2 was bubbled over the Pt cathode, and H_2 was bubbled over the Pt anode, and the resulting polarization curve is shown in Figure 5D. At all currents, the cell potential exceeded that achievable using the single-pH system. Note, in particular, the very high potential at low currents (1.82 V at 5.78 mA cm^{-2}), in excess of the thermodynamic maximum of a conventional fuel cell when the anode and cathode are in solutions of the same pH (1.229 V). If the anode and cathode are in solutions of different pH values, the thermodynamic maximum voltage increases by 0.059 V × pH difference at room temperature. The higher cell potential of the dual-pH system led to a much higher peak power density of that cell (~4.5 mW cm^{-2} at about 6 mA cm^{-2}) than of the single-pH system. We did find during our investigations that some Ag metal dissolved from the bipolar electrode and deposited on the Pt electrodes if the cell was run for a long time. Therefore, while this system acts as a proof-of-principle, and demonstrates the opportunities offered by combining CBEs and different-pH electrolytes, further work is needed to develop a more stable CBE for use in such systems. Moreover the development of such a CBE system could negate the need for any membranes within our devices.

Conclusions

We have shown that it is possible to separate the gases evolved from electrolytic water splitting by using a CBE in contact with dissolved, reversible redox species (instead of an ionically-conducting electrolyte to bridge the H_2- and O_2-evolution compartments). By integrating such systems into electrolysers, the devices could run safely at much lower current densities than typical devices can, increasing the viability of energy storage devices connected to wind turbines and solar panels. Future iterations of our device will benefit from the use of CBEs that negate the need for membranes separating the CBE from the H_2- and O_2-evolving

electrodes. We have also demonstrated a proof-of-concept fuel cell that, due to the spatial separation afforded by the use of the CBE, can maintain two different pH values at the cathode and anode. If a stable bipolar electrode were found, then a fuel cell with an open-circuit potential near 2.057 V could potentially be made, increasing the device power output. However, significant cell-engineering design considerations must be made before such a system can be realized. Finally, we note that the use of Ag/AgCl electrodes as the CBE eliminates the requirement for any membranes in our fuel cell device. This raises the possibility of developing a H_2/Cl_2 fuel cells using such a bipolar system. H_2/Cl_2 fuel cells are more efficient than H_2/O_2 fuel cells but suffer from the damage of membranes by Cl_2,[37] so the concepts described here may go some way towards addressing this issue.

Experimental Section

All chemicals were from Sigma-Aldrich and were used as received. Electrochemical experiments were carried out using a CH760 potentiostat from CH Instruments (Austin TX). Glassy carbon, Au and Pt disk electrodes (diameters 3 mm, 2 mm, and 2 mm, respectively) were also from CH Instruments. A 0.5-mm diameter Pt wire and Pt flag electrode (surface areas ~ 0.8 cm^2) were used for water splitting. Disk electrodes were cleaned before use by polishing with alumina (0.3 and 0.05 μm), then rinsing with de-ionized water. Pt-wire and Pt-flag electrodes were cleaned by annealing in a butane flame. Carbon-cloth CBE electrodes were cut from carbon cloth (~15 cm in length) tied at one end to avoid fraying, and connected to each other by copper wire. Nafion membranes (183 μm thickness) were stored in solutions of 0.1 M KOH or 1.0 M H_2SO_4 between use. Impedance measurements were performed in the frequency range from 100 kHz to 0.1 Hz, at an amplitude of 5 mV, and 0.0 V applied potential, by sandwiching activated Nafion membranes between two Pt contact plates. Powder X-ray diffraction analysis was carried out using a PANanalytical X'Pert PRO

diffractometer with Cu-K_α radiation operating at 40 kV and 40 mA, with 0.02° step size and 30 s step time. SEM images were recorded using a Philips Model XL30 FEG environmental microscope operated at 20 kV. Mass spectrometry was carried out using a Pfeiffer Vacuum Thermostar Quadropole mass spectrometer. Ni_2P inks were prepared by adding 2.4 mg Ni_2P to 0.95 mL of ethanol and 50 μL of 5% Nafion. The mixture was sonicated for at least 30 minutes before pipetting the required volume onto a GC electrode and drying gently under air.

Acknowledgements

We thank the Engineering and Physical Sciences Research Council for funding through project EP/P002382/1 the Centre for Doctoral Training in Fuel Cells and their Fuels (Project EP/L015749/1). We also thank the Nottingham Nanoscale and Microscale Research Centre (NMRC) for access to microscopy facilities.

References

(1) Yang, Z. G.; Zhang, J. L.; Kintner-Meyer, M. C. W.; Lu, X. C.; Choi, D. W.; Lemmon, J. P.; Liu, J. Electrochemical Energy Storage for Green Grid. *Chem. Rev.* **2011**, *111*, 3577-3613.

(2) Whittingham, M. S. History, Evolution, and Future Status of Energy Storage. *Proc. IEEE* **2012**, *100*, 1518-1534.

(3) Lewis, N. S.; Nocera, D. G. Powering the planet: Chemical Challenges in Solar Energy Utilization. *Proc. Natl. Acad. Sci. USA* **2006**, *103*, 15729-15735.

(4) Shaner, M. R.; Atwater, H. A.; Lewis, N. S.; McFarland, E. W. A Comparative Technoeconomic Analysis of Renewable Hydrogen Production using Solar Energy. *Energy Environ. Sci.* **2016**, *9*, 2354-2371.

(5) Rand, D. A. J.; Dell, R. M. Hydrogen Energy: Challenges and Prospects; RSC Publishing: Cambridge, UK, 2008.

(6) Felgenhauer, M.; Hamacher, T. State-of-the-art of Commercial Electrolyzers and On-site Hydrogen Generation for Logistic Vehicles in South Carolina. *Int. J. Hydrogen Energy* **2015**, *40*, 2084-2090.

(7) Zeng, K.; Zhang, D. Recent Progress in Alkaline Water Electrolysis for Hydrogen Production and Applications. *Progr. Energy Combust. Sci.* **2010**, *36*, 307-326.

(8) Carmo, M.; Fritz, D. L.; Mergel, J.; Stolten, D. A Comprehensive Review on PEM Water Electrolysis. *Int. J. Hydrogen Energy* **2013**, *38*, 4901-4934.

(9) Wang, Y.; Leung, D. Y. C.; Xuan, J.; Wang, H. A Review on Unitized Regenerative Fuel Cell Technologies, Part-A: Unitized Regenerative Proton Exchange Membrane Fuel Cells. *Renew. Sust. Energy Rev.* **2016**, *65*, 961-977.

(10) Prabhakaran, V.; Arges, C. G.; Ramani, V. Investigation of Polymer Electrolyte Membrane Chemical Degradation and Degradation Mitigation using In Situ Fluorescence Spectroscopy. *Proc. Natl. Acad. Sci. USA* **2012**, *109*, 1029-1034.

(11) Millet, P.; Ngameni, R.; Grigoriev, S. A.; Fateev, V. N. Scientific and Engineering Issues Related to PEM Technology: Water Electrolysers, Fuel Cells and Unitized Regenerative Systems. *Int. J. Hydrogen Energy* **2011**, *36*, 4156-4163.

(12) Grigoriev, S. A.; Porembskiy, V. I.; Korobtsev, S. V.; Fateev, V. N.; Auprêtre, F.; Millet, P. High-pressure PEM Water Electrolysis and Corresponding Safety Issues. *Int. J. Hydrogen Energy* **2011**, *36*, 2721-2728.

(13) Chen, L.; Dong, X.; Wang, F.; Wang, Y.; Xia, Y. Base-Acid Hybrid Water Electrolysis. *Chem. Commun.* **2016**, *52*, 3147-3150.

(14) Hashemi, S. M. H.; Modestino, M. A.; Psaltis, D. A Membrane-less Electrolyzer for Hydrogen Production across the pH Scale. *Energy Environ. Sci.* **2015**, *8*, 2003-2009.

(15) Symes, M. D.; Cronin, L. Decoupling Hydrogen and Oxygen Evolution during Electrolytic Water Splitting using an Electron-coupled-proton Buffer. *Nat. Chem.* **2013**, *5*, 403-409.

(16) Rausch, B.; Symes, M. D.; Cronin, L. A Bio-Inspired, Small Molecule Electron-Coupled-Proton Buffer for Decoupling the Half-Reactions of Electrolytic Water Splitting. *J. Am. Chem. Soc.* **2013**, *135*, 13656-13659.

(17) Rausch, B.; Symes, M. D.; Chisholm, G.; Cronin, L. Decoupled Catalytic Hydrogen Evolution from a Molecular Metal Oxide Redox Mediator in Water Splitting. *Science* **2014**, *345*, 1326-1330.

(18) Chen, L.; Dong, X.; Wang, Y.; Xia, Y. Separating Hydrogen and Oxygen Evolution in Alkaline Water Electrolysis using Nickel Hydroxide. *Nat. Commun.* **2016**, *7*, 11741.

(19) Choi, B.; Panthi, D.; Nakoji, M.; Kabutomori, T.; Tsutsumi, K.; Tsutsumi, A. A Novel Water-splitting Electrochemical Cycle for Hydrogen Production using an Intermediate Electrode. *Chem. Eng. Sci*. **2017**, *157*, 200-208.

(20) Fosdick, S. E.; Knust, K. N.; Scida, K.; Crooks, R. M. Bipolar Electrochemistry. *Angew. Chem. Int. Ed.* **2013**, *52*, 10438-10456.

(21) Loget, G.; Zigah, D.; Bouffier, L.; Sojic, N.; Kuhn, A. Bipolar Electrochemistry: From Materials Science to Motion and Beyond. *Acc. Chem. Res.* **2013**, *46*, 2513-2523.

(22) Jiang, J.-Z.; Guo, M.-H.; Yao, F.-Z.; Li, J.; Sun, J.-J. Propulsion of Copper Microswimmers in Folded Fluid Channels by Bipolar Electrochemistry. *RSC Adv.* **2017**, *7*, 6297-6302.

(23) Mavre, F.; Anand, R. K.; Laws, D. R.; Chow, K.-F.; Chang, B.-Y.; Crooks, J. A.; Crooks, R. M. Bipolar Electrodes: A Useful Tool for Concentration, Separation, and Detection of Analytes in Microelectrochemical Systems. *Anal. Chem.* **2010**, *82*, 8766-8774.

(24) Eßmann, V.; Barwe, S.; Masa, J.; Schuhmann, W. Bipolar Electrochemistry for Concurrently Evaluating the Stability of Anode and Cathode Electrocatalysts and the Overall Cell Performance during Long-Term Water Electrolysis. *Anal. Chem.* **2016**, *88*, 8835-8840.

(25) Millet, P.; Mbemba, N.; Grigoriev, S. A.; Fateev, V. N.; Aukauloo, A.; Etiévant, C. Electrochemical Performances of PEM Water Electrolysis Cells and Perspectives. *Int. J. Hydrogen Energy* **2011**, *36*, 4134-4142.

(26) Lukowski, M. A.; Daniel, A. S.; Meng, F.; Forticaux, A.; Li, L.; Jin, S. Enhanced Hydrogen Evolution Catalysis from Chemically Exfoliated Metallic MoS_2 Nanosheets. *J. Am. Chem. Soc.* **2013**, 135, 10274-10277.

(27) McKone, J. R.; Sadtler, B. F.; Werlang, C. A.; Lewis, N. S.; Gray, H. B. Ni–Mo Nanopowders for Efficient Electrochemical Hydrogen Evolution. *ACS Catal.* **2013**, *3*, 166-169.

(28) Faber, M. S.; Jin, S. Earth-abundant Inorganic Electrocatalysts and their Nanostructures for Energy Conversion Applications. *Energy Environ. Sci.* **2014**, *7*, 3519-3542.

(29) May, K. J.; Carlton, C. E.; Stoerzinger, K. A.; Risch, M.; Suntivich, J.; Lee, Y.-L.; Grimaud, A.; Shao-Horn, Y. Influence of Oxygen Evolution during Water Oxidation on the Surface of Perovskite Oxide Catalysts. *J. Phys. Chem. Lett.* **2012**, *3*, 3264-3270.

(30) Popczun, E. J.; McKone, J. R.; Read, C. G.; Biacchi, A. J.; Wiltrout, A. M.; Lewis, N. S.; Schaak, R. E. Nanostructured Nickel Phosphide as an Electrocatalyst for the Hydrogen Evolution Reaction. *J. Am. Chem. Soc.* **2013**, *135*, 9267-9270.

(31) Kucernak, A. R. J.; Sundaram, V. N. N. Nickel Phosphide: The Effect of Phosphorus Content on Hydrogen Evolution Activity and Corrosion Resistance in Acidic Medium. *J. Mater. Chem. A* **2014**, *2*, 17435-17445.

(32) Stern, L. A.; Feng, L. G.; Song, F.; Hu, X. L. Ni_2P as a Janus Catalyst for Water Splitting: The Oxygen Evolution Activity of Ni_2P Nanoparticles. *Energy Environ. Sci.* **2015**, *8*, 2347-2351.

(33) Marković, N. M.; Ross, P. N. Surface Science Studies of Model Fuel Cell Electrocatalysts. *Surf. Sci. Rep.* **2002**, *45*, 121-229.

(34) Debe, M. K. Electrocatalyst Approaches and Challenges for Automotive Fuel Cells. *Nature* **2012**, *486*, 43-51.

(35) Larminie, J.; Dicks, A. Fuel Cell Systems Explained; Second ed.; John Wiley & Sons Ltd: Chichester, 2003.

(36) Cohen, J. L.; Volpe, D. J.; Westly, D. A.; Pechenik, A.; Abruna, H. D. A Dual Electrolyte H_2/O_2 Planar Membraneless Microchannel Fuel Cell System with Open Circuit Potentials in excess of 1.4 V. Langmuir **2005**, *21*, 3544-3550.

(37) Thomassen, M.; Sandnes, E.; Borresen, B.; Tunold, R. Evaluation of Concepts for Hydrogen - Chlorine Fuel Cells. *J. Appl. Electrochem.* **2006**, *36*, 813-819.